Focal adhesion proteins connect IgE receptors to the cytoskeleton as revealed by micropatterned ligand arrays

Alexis J. Torres, Lavanya Vasudevan, David Holowka, and Barbara A. Baird[1]

Department of Chemistry and Chemical Biology, Cornell University, Ithaca, NY 14853

Patterned surfaces that present specific ligands in spatially defined arrays are used to examine structural linkages between clustered IgE receptors (IgE-FcεRI) and the cytoskeleton in rat basophilic leukemia (RBL) mast cells. We showed with fluorescence microscopy that cytoskeletal F-actin concentrates in the same regions as cell surface IgE-FcεRI that bind to the micrometer-size patterned ligands. However, the proteins mediating these cytoskeletal connections and their functional relevance were not known. We now show that whereas the adaptor proteins ezrin and moesin do not detectably concentrate with the array of clustered IgE-FcεRI, focal adhesion proteins vinculin, paxillin, and talin, which are known to link F-actin with integrins, accumulate in these regions on the same time scale as F-actin. Moreover, colocalization of these focal adhesion proteins with clustered IgE-FcεRI is enhanced after addition of fibronectin-RGD peptides. Significantly, the most prominent rat basophilic leukemia cell integrin (α5) avoids the patterned regions occupied by the ligands and associates preferentially with exposed regions of the silicon substrate. Thus, spatial separation provided by the patterned surface reveals that particular focal adhesion proteins, which connect to the actin cytoskeleton, associate with ligand-cross-linked IgE-FcεRI, independently of integrins. We investigated the functional role of one of these proteins, paxillin, in IgE-FcεRI-mediated signaling by using small interfering RNA. From these results, we determine that paxillin reduces stimulated phosphorylation of the FcεRI β subunit but enhances stimulated Ca^{2+} release from intracellular stores. The results suggest that paxillin associated with clustered IgE-FcεRI has a net positive effect on FcεRI signaling.

FceRI | Lyn | nanobiotechnology | paxillin | supported lipid bilayers

Cells have evolved to respond to their chemical and physical environment. Chemical stimulants in the form of soluble or surface-bound ligands are recognized by specific cell surface receptors, and physical cues are sensed by integrins that bind to extracellular matrix proteins on surrounding substrates (1). Cross-talk between intracellular signaling pathways that are initiated by integrins and by ligand receptors has been clearly demonstrated, although spatial aspects of these processes have not been defined. Surfaces patterned on the micrometer scale offer the opportunity to separate regions that bind integrins from those that present ligands to cell surface receptors and thereby delineate respective cytoskeletal connections.

The subject of our study is the IgE receptor (FcεRI), which is a member of the family of multisubunit immune recognition receptors that includes antigen receptors on B cells and T cells. This family of receptors has conserved structural features and similarly initiates intracellular signaling in response to multivalent ligands (antigens) that activate cells by clustering cell surface receptors. FcεRI receptors are found primarily in mast cells and basophils and are sensitized to a particular antigen by high-affinity binding of IgE with the corresponding specificity. Cross-linking of IgE-FcεRI by antigen triggers intracellular signaling events, leading to multiple cellular responses, including degranulation to release chemical

mediators that cause inflammatory and allergic reactions. In the earliest signaling events, antigen-induced clustering of IgE-FcεRI causes stable association with ordered lipid domains, wherein the tyrosine kinase Lyn phosphorylates the FcεRI β and γ subunits, resulting in recruitment and activation of tyrosine kinase Syk (2, 3). Activated Syk phosphorylates a series of proteins resulting in Ca^{2+} mobilization and other downstream signaling steps leading to degranulation.

We recently examined spatial relationships during IgE-FcεRI-mediated signal transduction by using microfabricated ligand arrays. The patterned ligands cause spatially defined clustering of IgE-FcεRI on the cell surface which, because the IgE binds to the ligands, corresponds to the same pattern. These patterned ligands and binding receptors can be visualized with fluorescence microscopy; the periodicity of the patterns enables reliable and quantitative evaluation of localized receptors and signaling components that coredistribute.

We showed with patterned lipid bilayers containing 2,4-dinitrophenyl (DNP) ligands that tyrosine kinase activity (as visualized with anti-phosphotyrosine antibodies) occurs in the liganded regions on the same time scale that anti-DNP IgE-FcεRI clusters in those regions, and detectable accumulation of the Lyn-GFP kinase occurs after ≈15 min. Cytoskeletal F-actin visually concentrates in these regions after ≈30 min. Notably, cytochalasin D, which inhibits actin polymerization, prevents the micrometer-scale accumulation of Lyn but not the initial tyrosine phosphorylation (4), supporting the view that the actin cytoskeleton becomes involved as signaling progresses.

The present work examines the reorganization and the regulatory role of the actin cytoskeleton during FcεRI-mediated signal transduction, and we focus on participation of several actin-binding proteins that have been examined in other signaling pathways. In particular, we investigate ezrin and moesin, which have been implicated in T cell receptor signaling, and paxillin, vinculin, and talin, which are known to be involved in focal adhesion complexes and participate in integrin-mediated signaling (5). The adaptor protein paxillin has several binding sites for Src kinases that are relevant in immune cell signaling (6).
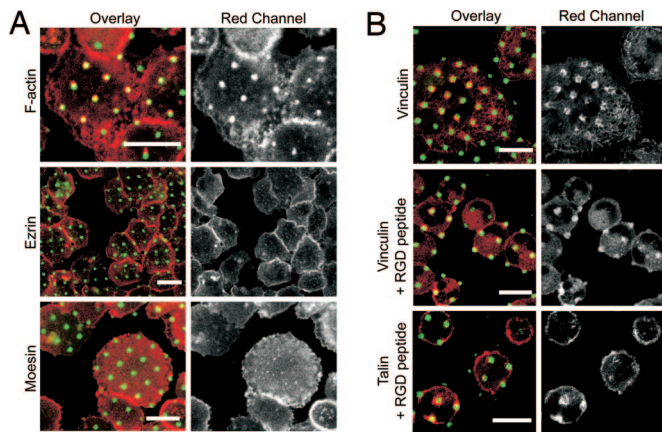
Fig. 1. Vinculin and talin, but not ezrin and moesin, visibly coredistribute with clustered IgE-FcεRI. Confocal florescence micrographs show cells incubated at 37°C with patterned lipid bilayers containing DNP-cap-PE and stained for specific intracellular proteins (red). Clustered IgE-FcεRI on cell surfaces are visualized by Alexa Fluor 488-labeled IgE (green). (A) F-actin accumulates consistently with the clustered FcεRI-IgE, whereas ERM family members, ezrin and moesin, do not. (B) Focal adhesion proteins vinculin and talin redistribute with clustered IgE-FcεRI in the absence and presence of fibronectin-RGD peptides (RGDSP or RGDSPT). Intracellular proteins were labeled after ≈40-min incubation of cells with substrates, followed by cell fixation and treatment with Alexa Fluor 568 phalloidin (F-actin) or specific antibodies (ezrin, moesin, vinculin, talin). (Scale bars: 20 μm.)

Previous studies on rat basophilic leukemia (RBL) mast cells showed that paxillin is tyrosine-phosphorylated after activation of IgE-FcεRI by multivalent ligand (7). Another study identified paxillin as a protein precipitated by a maltose binding protein-Lyn fusion protein only after ligand-mediated clustering of IgE-FcεRI in RBL mast cells, suggesting that this protein is involved in signaling events downstream of the initial phosphorylation of FcεRI (8). Our present work with patterned ligands shows that focal adhesion proteins vinculin, talin, and paxillin coredistribute with clustered IgE-FcεRI independently from integrins and thereby provide a direct link to the actin cytoskeleton. Moreover, use of short interfering RNA (siRNA) to knock down paxillin expression shows that paxillin plays a regulatory role in IgE-FcεRI signaling. Thus, micropatterned ligand arrays, together with biological manipulation of cellular components, reveals spatially distinctive control of cell signaling by receptors and integrins.

Results

F-actin in RBL Cells Redistributes Reversibly with IgE-FcεRI That Are Clustered by Micropatterned Ligands.
We labeled F-actin with Alexa Fluor 568 phalloidin at various time points after incubating anti-DNP IgE-sensitized RBL cells with the substrates at 37°C. Consistent with our previous results obtained with actin-EGFP (4), we observed accumulation of the actin label over the patterned features after 25-min stimulation (Fig. 1A), and the percentage of cells showing clear actin patches became maximal (typically 70% of the cells) after ≈40 min. These patches are observed on top of a diffuse background of cortical actin stain, and some day-to-day variability of detected colocalization with the patterned bilayers is caused by this background fluorescence. We investigated the specificity and stability of visibly coclustered IgE-FcεRI and cytoskeletal actin by adding 20 μM DNP-aminocaproyl-L-tyrosine 25–30 min after the initial incubation of cells with the patterned bilayers. This soluble monovalent DNP-ligand competes with the immobilized 1,2-dipalmitoyl-sn-glycero-3-phosphoethanolamine-N-[6-[(2,4-dinitrophenyl)amino]caproyl] (DNP-cap-PE) in the lipid bilayers and causes the

clustered IgE-FcεRI to disperse within 30 min (data not shown). The coincident F-actin stain also disperses on the same time scale as the clustered IgE-FcεRI as monitored in live cells transfected with actin-EGFP [supporting information (SI) Fig. S1]. These results demonstrate that cytoskeletal actin coredistribution occurs specifically with clustered IgE-FcεRI and is reversible, pointing to the presence of connecting proteins that sense the state of IgE-FcεRI aggregation.

Pretreatment of cells with inhibitors of actin polymerization such as cytochalasin D prevents coredistribution of F-actin with IgE-FcεRI that is clustered by patterned ligands, as shown in ref. 4. In contrast, we find that colocalized IgE-FcεRI and F-actin patches, as reported by actin–EGFP on live cells, are not reversed if cytochalasin D (4 μM) is added after these patches are formed (Fig. S1). These results indicate the polymerized actin associated with the clustered receptors forms stable structures, probably by means of proteins that cross-link F-actin.

We evaluated members of the ezrin/radixin/moesin (ERM) family that are involved in coupling some signaling components in the plasma membrane with the actin cytoskeleton (9). In particular, ERM adaptors have been implicated in regulation of the immunological synapse in T cells (10). Antibodies specific for either ezrin or moesin were added to cells that had been fixed after incubation with the patterned ligands for periods up to 1 h, followed by fluorescent secondary antibody. Although a diffuse membrane stain could be seen, no concentration of anti-ezrin or anti-moesin with the pattern of clustered IgE-FcεRI was detected in numerous experiments of this type (Fig. 1A).

Focal Adhesion Proteins Coredistribute with Clustered IgE-FcεRI.
Vinculin, talin, and paxillin are involved in complexes associated with focal adhesions that form when integrins bind to extracellular matrix (ECM) proteins, such as fibronectin, and consequently form linkages to the cytoskeleton (5). With antibodies specific for vinculin and talin we observed recruitment of both of these proteins to the patches of IgE-FcεRI that form in RBL cells after incubation with the patterned, liganded substrates. The kinetics of this accumulation is very similar to that of F-actin: resolvable patches of vinculin or talin appear after ≈25 min and become maximal after ≈40 min (Fig. 1B). The number of cells with detectable patches of talin, typically 25%, is less than that for vinculin, typically 70%, and this finding may be caused by differences in antibodies or different levels of specific background staining that affects contrast. The stain that concentrates with the patches sometimes appears ring-like, suggesting limited accessibility.

RBL cells adhere to and spread on glass possibly by means of fibronectin or other ECM proteins secreted by these cells, and attached cells labeled with anti-vinculin exhibit structures resembling focal adhesions (see Fig. S4). On substrates patterned with lipid bilayers, the cells adhere in regions between the patterned features. To test dependence of IgE-FcεRI, vinculin, and talin clustering on integrin engagement and activation, we used soluble RGD peptides that compete with fibronectin-binding sites. We found that addition of 0.5–1 mg/ml GRGDSP or GRGDPT peptides, known to inhibit integrin-mediated cellular attachment (11), causes reduced cell spreading on the substrate, but this treatment does not prevent patches of vinculin and talin in regions of the pattern ligands (Fig. 1B). On the contrary, we find that this treatment increases the accumulation of these focal adhesion proteins in these regions, probably because they have been released from integrin complexes.

Control experiments and quantitative analyses were carried out. Direct comparison of patterned lipid bilayers containing or not containing the DNP-cap-PE ligand showed that vinculin and talin coredistribute with IgE-FcεRI only when the specific ligand is present (Fig. S2). In other experiments, patterned lipid bilayers were replaced by patterned BSA conjugated to DNP (DNP-
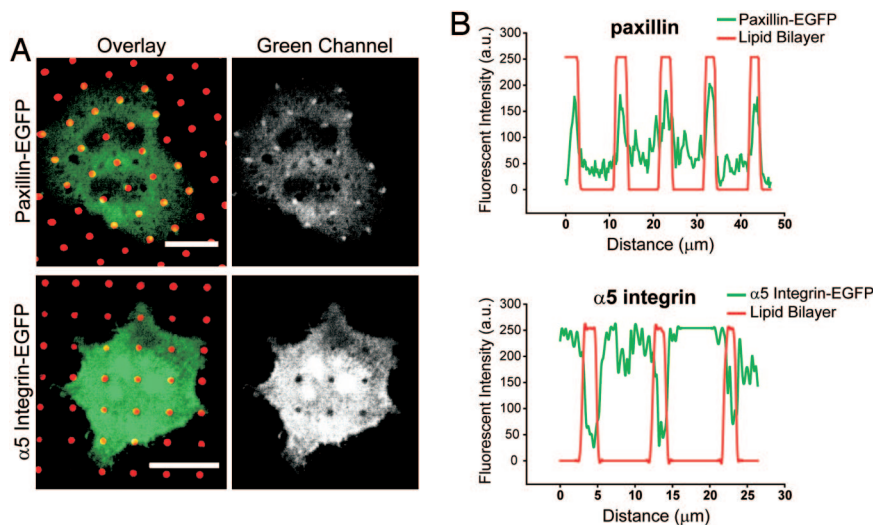
Fig. 2. Paxillin coredistributes with clustered IgE-FcεRI and patterned lipid bilayers, but integrins avoid these regions. Confocal micrographs show cells expressing paxillin-EGFP or integrin α5-EGFP (green) after incubation for 40 min at 37°C with patterned lipid bilayers (red) containing DNP-cap-PE and fixation before imaging. (*A*) Paxillin is recruited with IgE-FcεRI in the regions of patterned ligands, and α5-integrin is excluded. (Scale bars: 20 μm.) (*B*) Intensity line profiles from images in *A* confirm that paxillin accumulation and integrin exclusion correspond exactly to where the patterned bilayers are localized.

BSA) by using the same lithographic mask and Parylene liftoff method. These substrates were tested with RBL cells sensitized or not with anti-DNP IgE, and vinculin, paxillin, ezrin, or moesin was fluorescently labeled. None of these markers clustered with the patterned DNP-ligand for cells without IgE bound to FcεRI, whereas vinculin and paxillin but not ezrin or moesin formed patterned clusters on cells with bound IgE. Cross-correlation analysis provides quantitative confirmation of these results (Fig. S3)

We investigated whether the association of actin and focal adhesion protein vinculin with clustered IgE-FcεRI is affected by early signaling activities stimulated by these receptors. We treated cells with two different inhibitors of Syk kinase that is activated by clustered IgE-FcεRI after receptor phosphorylation by Lyn kinase (12). Addition of Syk inhibitor SI (1 μM) (13) or piceatannol (40 μM) before and during incubation of cells with liganded substrates had no detectable effect on redistribution of vinculin or actin with the clustered receptors. The same concentrations of these Syk inhibitors reduce antigen-stimulated degranulation by 75–80%. We also tested PP1 (15 μM), which inhibits Lyn and other Src family kinases, and this inhibitor reduced by half the percentage of cells showing coredistribution of actin or vinculin with clustered receptors. Cytochalasin D (2 μM) completely abrogates F-actin recruitment, as described above, and this treatment similarly prevents patching of vinculin with clustered receptors. Our results with these inhibitors indicate that vinculin and actin redistribution with clustered IgE-FcεRI depends in part on Src family kinase activity but not on Syk activity.

We considered whether the accumulation of these focal adhesion proteins depends on mechanical tension induced by nonmuscle myosin II, a motor protein involved in regulation and distribution of actin filaments such as occurs during formation of stress fibers. As a test, we treated cells with blebbistatin, an inhibitor of myosin II ATPase activity, at a concentration of 50 μM before and during 40-min incubation of cells with patterned DNP-ligands. This treatment decreased filamentous heterogeneity of fluorescently labeled vinculin or paxillin and enhanced rather than reduced coredistribution of actin (data not shown), vinculin, or paxillin with clustered IgE-FcεRI compared with samples without blebbistatin (Fig. S3 *A, B,* and *D*).

Paxillin Coredistributes with Clustered IgE-FcεRI Independently of Integrins. Paxillin is known to connect vinculin with other binding partners in focal adhesion complexes (Fig. S4). We transfected RBL cells with the gene construct for paxillin-EGFP and observed coredistribution of the expressed protein with clustered IgE-FcεRI after cells were incubated with patterned substrates (Fig. 2). Clear patches of paxillin-EGFP emerged above the background level in many cells, typically in ≈35% after 40 min. In other experiments when anti-paxillin was used as the label, typically 70% of the cells showed coclustering with IgE-FcεRI (Fig. S3).

As described in a previous section, we observed that soluble RGD peptides enhanced accumulation of vinculin and talin with clustered IgE-FcεRI (Fig. 1*B*). To investigate further whether these interactions of focal adhesion proteins are independent of integrin engagement and signaling, we evaluated RBL cells expressing a GFP construct of α5-integrin and compared these in the same experiment with cells expressing paxillin-EGFP. In contrast to paxillin, α5-integrin resists association with the lipid bilayer regions that contain the specific ligand DNP-cap-PE. This difference is striking in the images and can be quantified with line scans (Fig. 2). Tested in several independent experiments, as many as 65% of cells expressing the EGFP-labeled integrin showed this exclusion, and concentration of this protein was never observed in the patterns. None of the other samples containing IgE-sensitized cells with labeled vinculin, talin, or paxillin ever showed this exclusion in many different experiments with the liganded arrays of lipid bilayers. This aversion of α5-integrin to the patterned regions is not caused by clustering and activation of the IgE receptors because the same occurs when the ligand, DNP-cap-PE, is not included in the lipid bilayers (data not shown).

Functional Role of Paxillin in IgE-FcεRI Signaling. Our observation of paxillin clustering with IgE-FcεRI on patterned bilayers, together with previous evidence that paxillin is involved in FcεRI-mediated signaling (see Introduction), prompted us to examine more directly the functional importance of this adaptor protein. For this purpose, we used siRNA to knock down expression of endogenous paxillin. Two different siRNA constructs caused >90% reduction of paxillin (Fig. 3*A*). To evaluate participation of paxillin in coredistribution of F-actin with clustered IgE-
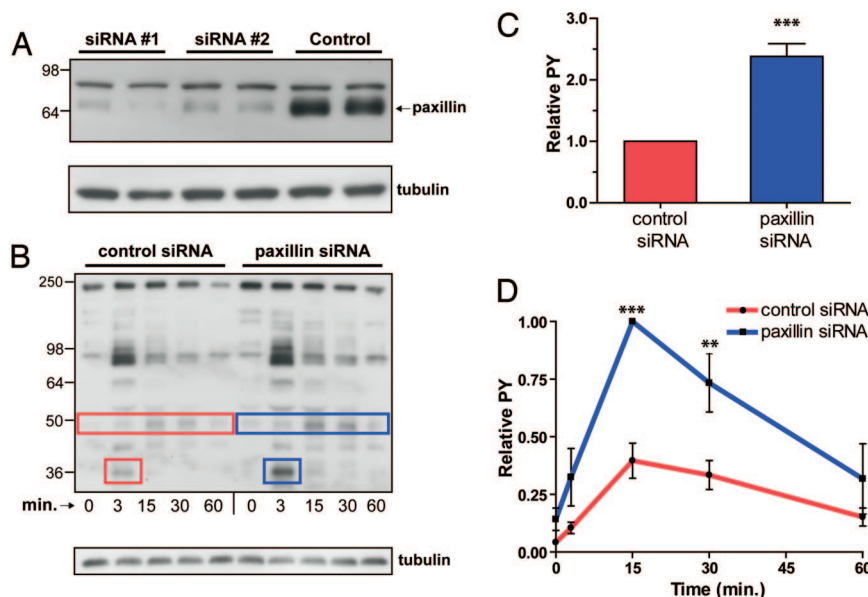
Fig. 3. Paxillin knockdown affects phosphorylation stimulated by IgE-FcεRI. (*A*) Immunoblots show that paxillin-specific siRNA causes >90% decrease in paxillin expression levels. To confirm knockdown, the same PDVF membrane was stripped and reprobed with anti-tubulin as a loading control. (*B*) Antigen-stimulated phosphorylation was examined in lysates from suspended whole cells (2×10^6/ml) 48 h after siRNA delivery, sensitization with anti-DNP IgE, and stimulation with DNP-BSA (50 ng/ml) for the times indicated. After SDS/PAGE, gels were blotted with anti-phosphotyrosine antibody, 4G10. Boxes indicate 35-kDa (p35) and 50-kDa (p50) bands that are consistently increased after paxillin knockdown in this representative experiment; anti-tubulin bands serve as loading control. (*C*) Densitometric analysis of tyrosine phosphorylation (PY) for p35 band (FcεRI β) after 3-min stimulation. (*D*) Densitometric plot showing stimulation time course for relative tyrosine phosphorylation of the p50 band. (*C* and *D*) Data are averaged over five different experiments in which the phosphorylated band was normalized by tubulin band (loading control). The data were further normalized to control (sham knockdown) cells (*C*) or to the 15-min time point in the knockdown cells (*D*). ∗∗, $P < 0.01$; ∗∗∗, $P < 0.001$. Error bars indicate S.E.M.

FcεRI, we stained knockdown and control cells with Alexa Fluor 568 phalloidin after a 40-min incubation with the patterned ligands. We detected no differences, indicating that although paxillin may be involved in linking clustered receptors to the cytoskeleton, it is not essential.

Measurements of receptor-mediated cellular responses were carried out on suspended cells to eliminate signaling effects caused by integrin-mediated binding to substrates. We evaluated effects of paxillin knockdown on tyrosine phosphorylation stimulated by IgE-FcεRI by incubating suspended cells with multivalent ligand (DNP-BSA) and immunoblotting cell lysates with an anti-phosphotyrosine antibody. Paxillin knockdown cells yielded a pattern of stimulated tyrosine phosphorylation that was qualitatively similar to control cells treated with nonspecific siRNA (Fig. 3*B*). However, the knockdown cells showed a clear and consistent increase in phosphorylation of two bands corresponding to molecular masses of 35 kDa (p35) and 50 kDa (p50) (Fig. 3 *B–D*). The p35 band corresponds to FcεRI β, as demonstrated (14); consistent with this assignment the phosphorylation of this band is maximal 3 min after the cells are stimulated with multivalent ligand at 37°C. In contrast, tyrosine phosphorylation of the p50 band is maximal 15 min after stimulation. The time course of phosphorylation of p50 is consistent with it being a substrate of Csk kinase that negatively regulates Src kinases (15). These results with the knockdown cells suggest that paxillin, possibly by binding to Lyn, plays a negative regulatory role in Lyn phosphorylation of the p35 and p50 substrates.

We also evaluated downstream steps of activation in the paxillin knockdown cells. Stimulated Ca^{2+} mobilization, which follows after initial FcεRI phosphorylation and precedes cellular degranulation, occurs in two phases: release from intracellular stores and influx from extracellular medium. In buffer containing Ca^{2+}, the paxillin knockdown cells show a small but consistent decrease in the Ca^{2+} response (Fig. 4*A*). To evaluate separately the stimulated Ca^{2+} release from stores and Ca^{2+}

influx, antigen was added in buffer containing no Ca^{2+}, and then Ca^{2+} was added subsequently. Paxillin knockdown cells showed a consistent decrease of ≈50% in stimulated Ca^{2+} release from the intracellular stores and a decrease of ≈10% in the Ca^{2+} influx (Fig. 4 *B* and *C*). These results are consistent with a negative regulatory effect of paxillin on Lyn-mediated activation of Csk or another negative regulator, which would result in an enhancing effect on antigen-stimulated Ca^{2+} release from stores.

Discussion

The patterned lipid bilayer substrate we used in this work restricts integrin-mediated adhesion to nonliganded regions, and this spatial separation reveals that actin-binding proteins vinculin, talin, and paxillin interact with ligand-clustered IgE-FcεRI in mast cells, independently of integrins. Our results suggest that these characteristic focal adhesion proteins serve to connect clustered IgE-FcεRI to cytoskeletal actin, which also coredistributes with these receptors and may regulate receptor-mediated signaling. We and others demonstrated the versatility of patterned ligands that confine and activate receptors in micrometer-size regions so that the spatially regulated cellular responses can be monitored (for review, see ref. 16). An important feature of patterned lipid bilayers is that proteins do not adhere nonspecifically to the lipid regions: anti-DNP IgE-FcεRI binds selectively to these regions only because DNP-cap-PE is incorporated in the bilayers (17). In contrast, the most prominent RBL cell integrin (α5) avoids the regions of the lipid bilayers and binds to the glass surface by means of ECM proteins secreted by the cells. Others also showed that supported lipid bilayers are resistive to protein absorption and cell adhesion (18).

Our experiments indicating that characteristic focal adhesion proteins connect antigen-clustered IgE-FcεRI to the cytoskeleton provide insight to increasing evidence for cytoskeletal regulation of FcεRI signaling (19–23). We showed that F-actin coconcentrates with IgE-FcεRI that is clustered in patches by
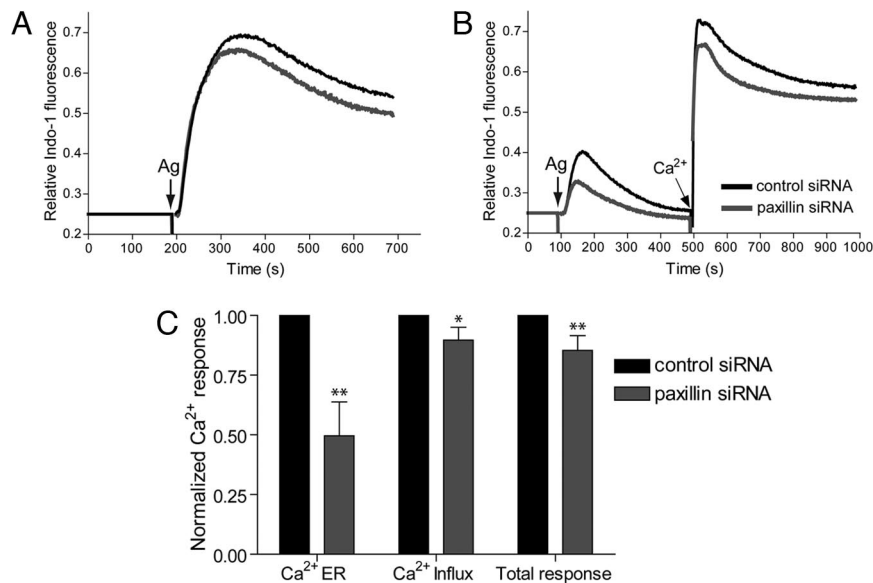
Fig. 4. Paxillin knockdown affects Ca^{2+} mobilization stimulated by IgE-FcεRI. Intracellular Ca^{2+} changes in paxillin knockdown (gray) and sham knockdown (black) cells after stimulation by DNP-BSA (50–200 ng/ml) at 37°C, in representative (*A* and *B*) and summarized (*C*) experiments. (*A*) Cells were stimulated in buffer containing 2 mM Ca^{2+}; release from intracellular stores and influx from the extracellular medium occurs under these conditions. (*B*) Cells were stimulated in the absence of extracellular Ca^{2+} such that only release from stores occurs; after 500 s the Ca^{2+} concentration in the buffer is increased to 2 mM (by addition of $CaCl_2$) such that influx occurs. (*C*) Averages over five experiments similar to that shown in *B*. The first two sets of two bars correspond to curves before and after addition of extracellular Ca^{2+} (2 mM), respectively; the last set corresponds to both curves additively. In each case, changes in intracellular Ca^{2+} concentration were integrated >500 s and normalized to the control cell response. *, $P < 0.05$; **, $P < 0.01$. Error bars indicate S.E.M.

immobilized DNP-ligands. This coredistribution is prevented, but not reversed, by cytochalasin D, suggesting stabilization of the polymerized F-actin by actin-binding proteins. In contrast, both IgE-FcεRI clustering and coconcentrating F-actin are reversed by soluble multivalent ligand that competes with the immobilized DNP-ligand. This dynamic, reversible process indicates that the linkage to the cytoskeleton is based on complexes forming stably with FcεRI only after oligomerization by multivalent ligand binding.

To investigate the composition of complexes that connect to the cytoskeleton, we examined several known actin-binding proteins. We detected no coredistribution of ezrin and moesin when sensitized cells are incubated with patterned ligands, in contrast to clear coredistribution of vinculin, talin, and paxillin. Moreover, these latter proteins accumulate visibly in the same patterns as the clustered IgE-FcεRI with kinetics similar to that observed for F-actin. Interactions among paxillin, vinculin, talin, and actin have been established in the context of integrin-based focal adhesion complexes (5, 24): Vinculin binds directly to paxillin and actin, whereas talin binds actin and vinculin as a result of integrin engagement. The patterned substrates revealed that complexes containing these components form in regions of clustered IgE-FcεRI, even when integrins (as represented by $\alpha5$) are excluded from these regions.

Our finding that Syk inhibitors, SI and piceatannol, do not inhibit vinculin and actin accumulation whereas the Src family tyrosine kinase, PP1, partially inhibits both suggests that the linkage between FcεRI and the cytoskeleton is enhanced by stimulated Lyn kinase activity and occurs before activation of Syk substrates or in parallel signaling pathways. Paxillin is tyrosine-phosphorylated after antigen activation in RBL mast cells (7) and has been found to interact with Lyn kinase in this and several other cell types (8, 25, 26), suggesting that paxillin is one of the proteins that provides a link to vinculin, talin, and thereby to the actin cytoskeleton.

The observed interactions of focal adhesion proteins with clustered IgE-FcεRI also lend insight to apparent signaling

cross-talk between these receptors and integrins. For example, it is known that adherence of RBL-2H3 cells to fibronectin-coated surfaces enhances degranulation and serves as a costimulus for cytokine production (27–29). Similarly, cell activation by antigen-mediated clustering of IgE-FcεRI causes increased adhesion and spreading in mast cells (30, 31). We demonstrated competing binding sites for focal adhesion proteins: soluble RGD peptides compete with immobilized fibronectin and bind integrins, consequently releasing vinculin and talin to increase their concentration with the clustered IgE-FcεRI.

The spatially distinctive information provided by the micropatterned ligand arrays is complemented with cell biological experiments. We found that substantially reducing paxillin in RBL cells with siRNA clearly enhances tyrosine phosphorylation of two proteins in response to stimulation by multivalent ligand: The p35 band we can identify as FcεRI β subunit, and the unidentified p50 band. Enhanced phosphorylation of FcεRI β stimulated by antigen was also seen for RBL cells treated with inhibitors of actin polymerization, cytochalasin D, and latrunculin (19, 20, 22). These results are consistent with the view that negative regulation of Lyn kinase mediated by paxillin (possibly by linking to the cytoskeleton) occurs during early stages of IgE-FcεRI signaling, when Lyn phosphorylates FcεRI β and γ subunits after antigen-mediated clustering of these receptors (32). This inhibitory effect of paxillin is also evident at later stages because of altered phosphorylation of the p50 protein, which may be a substrate of CSK or another negative regulatory kinase. Suppression by paxillin results in enhanced downstream signaling, as manifested by enhanced Ca^{2+} mobilization.

Paxillin knockdown cells showed only a small inhibitory effect on stimulated degranulation (Fig. S5), which is one end point of the cellular response. This result is not surprising because of the relatively modest inhibition of total Ca^{2+} mobilization. It is possible that other proteins compensate for paxillin knockdown or that paxillin plays a larger regulatory role in other stimulated cellular responses, such as cytokine production. In this regard, leupaxin (a member of the paxillin family of adaptor proteins) recently was

shown to regulate cytokine production resulting from B cell receptor signaling (26). Paxillin knockdown in RBL cells did not detectably affect F-actin coredistribution with clustered IgE-FcεRI on patterned bilayers, indicating that other proteins are also involved in these linkages, and these may have other regulatory effects. As demonstrated in this work, candidate proteins can now be examined with patterned substrates, pharmacological and genetic manipulation, and biological measurements.

Experimental Procedures

Materials. 1-Palmitoyl-2-oleoyl-sn-glycero-3-phosphocholine (POPC), DNP-cap-PE, and 1,2-dioleoyl-*sn*-glycero-3-phosphoethanolamine-*N*-(lissamine rhodamine B sulfonyl) (lissamine rhodamine PE) were purchased from Avanti Polar Lipids. Mouse monoclonal anti-DNP IgE was purified as described in ref. 33 and fluorescently modified with Alexa Fluor 488 (Molecular Probes) according to the labeling kit instructions. Cytochalasin D, mouse anti-vinculin (clone hVIN-1), and mouse anti-talin (clone 8d4) antibodies were purchased from Sigma–Aldrich. Alexa Fluor 568 phalloidin was purchased from Molecular Probes. Syk kinase inhibitor 3-(1-methyl-1H-indol-3-yl-methylene)-2-oxo-2,3-dihydro-1H-indole-5-sulfonamide (SI), *trans*-3,3′,4,5′-tetrahydroxystilbene (piceatannol), (−)-blebbistatin, and RGD peptides, GRGDSP, and GRGDPT were purchased from Calbiochem. Monoclonal anti-phosphotyrosine clone 4G10 was obtained from Upstate Cell Signaling Solutions (Millipore), monoclonal anti-α-tubulin (clone .N.593) from U.S. Biologicals, and monoclonal anti-paxillin clone 349 from BD Biosciences. Rabbit anti-ezrin and anti-moesin antibodies were gifts from A. Bretscher (Cornell University, Ithaca, NY). Integrin α5-EGFP and avian paxillin-EGFP cDNA constructs were gifts from A. Horwitz (University of Virginia, Charlottesville, VA). Actin-EGFP was a gift from A. Jeromin (Allen Institute, Seattle, WA).

Microfabrication of Patterned Ligands by Polymer Liftoff. Surfaces were patterned with 1- to 5-μm features as described (4, 17), and no significant differences were observed over this length range. Most experiments used patterned lipid bilayers containing POPC, DNP-cap-PE (and sometimes lissamine rhodamine PE) and omitted the DNP-ligand as a specificity control (7, 8). For further evaluation, additional experiments used patterned BSA that was conjugated with DNP and a fluorescent marker. Additional details are provided in *SI Methods*.

Cell Culture and Transfection. RBL-2H3 cells were maintained in monolayer cultures and harvested with trypsin-EDTA (Invitrogen) 3–5 days after passage, as described in ref. 34. Cells were sensitized by overnight incubation at 37°C with Alexa Fluor 488-labeled IgE or unlabeled IgE (0.5 μg/ml). For some experiments, cells were transiently transfected with specified EGFP constructs by using Lipofectamine 2000 (Invitrogen). Cells were suspended in buffered saline solution [135 mM NaCl, 5.0 mM KCl, 1.8 mM CaCl$_2$, 1.0 mM MgCl$_2$, 5.6 mM glucose, 20 mM Hepes (pH 7.4)] containing 1 mg/ml BSA. In some experiments, cells were incubated with specific inhibitors or other agents at 37°C for 5 min before and during the time of incubation with patterned substrates.

Fluorescence Microscopy and Immunofluorescence. Cells suspended at a concentration of 10^6 cells per ml were added to a patterned substrate (8 × 8 mm) in the center of a 35-mm Petri dish with coverglass bottom (0.16–0.19 mm; MatTek). After the specified incubation at 37°C (20–45 min), cells were imaged directly (live-cell imaging), or they were fixed with 3.7% formaldehyde in PBS for 10 min followed by quenching with 10 mg/ml BSA in PBS. For immunofluorescence after fixation, cells were labeled with primary antibody at room temperature for 1 h. After washing with PBS/BSA (1 mg/ml), the Alexa Fluor 568-labeled secondary antibody was incubated with samples at room temperature for 1 h. Control samples, which had nonspecific mouse IgG as the primary antibody, were evaluated to confirm negligible nonspecific label and

bleedthrough from the other fluorescence channel. Six to 12 independent experiments were carried out for each fluorescently labeled cellular component (e.g., ezrin, moesin, vinculin, and others).

A Bio-Rad-MRC600-confocal head coupled with a Zeiss Axiovert 10 inverted microscope was used for confocal microscopy. A 522/DF35 filter set was used for simultaneous or sequential dual-color image acquisition with an oil-immersion ×63, 1.4 numerical aperture objective. Two milliliters of buffered saline solution/BSA (for live cell imaging) or PBS (for fixed cells) was added into the dish before inverting the chip for microscopy observation. Positive cells showed fluorescent patterns that matched the substrate with intensity in the overlapping patches at least three times greater than the background level. Visual and quantitative analysis of the images is detailed in *SI Methods*.

Knockdown of Paxillin with siRNA. Predesigned On-TARGETplus SMARTpool siRNA (siRNA 1) targeting rat paxillin (Dharmacon) was used to reduce paxillin expression levels in RBL-2H3 cells. The siRNA pool sense sequences were GGAACUUCUUCGAGCGGGAUU, CCAGAAGGGUUCCACGAGAUU, GGCA-AAGCCUACUGUCGGAUU, and GCGAGGAGGAACACGUCUAUU. An additional predesigned siRNA (Ambion) with the sequence GCUCCAGCAC-CAAAAAUUC (siRNA 2) was used to confirm the results from the functional assays. A siRNA (On-TARGETplus siCONTROL; Dharmacon) with the sequence UGGUUUACAUGUCGACUAA was used as the nonspecific (sham knockdown) control. For optimal delivery of siRNA, cells were resuspended in buffer [137 mM NaCl, 2.7 mM KCl, 1 MgCl$_2$, 5.6 mM glucose, 20 mM Hepes (pH 7.4)] at a concentration of $1 × 10^7$ cells per ml and, after addition of 1.5 nM siRNA, electroporated by using an exponential pulse at 280 V and 950 μF. Electroporation was carried out in a 4-mm cuvette by using a Gene Pulser Xcell electroporator system (Bio-Rad). After electroporation, cells were plated in medium at a 25–30% confluence and incubated at 37°C for 48 h. Protein knockdown was confirmed by immunoblotting.

Cell Lysis and Immunoblotting. Whole-cell lysates were prepared on ice by suspending cells in lysis buffer [5 mM *N*-ethylmaleimide, 1 mM Na$_3$VO$_4$, 5 mM Na$_2$P$_2$O$_7$, 50 mM NaF, 2 mM iodoacetate, 5 mM EDTA, 0.1% (vol/vol) Triton X-100, 50 mM NaCl, 50 mM Tris and 2% protease inhibitor mixture (Sigma), pH 7.6]. Lysates were centrifuged at 15,000 × *g* for 10 min at 4°C. The supernatant was mixed with Tris-glycine SDS buffer and boiled for 5 min. Samples were resolved on a 12% Tris-glycine polyacrylamide gel and transferred to an Immobilon-P membrane with a pore size of 0.45 μm (Millipore) by semidry transfer. Immunoblots were visualized with the Enhanced Chemiluminescence method by using the appropriate antibodies.

Antigen-Stimulated Degranulation. RBL cells ($1 × 10^6$ cells per well in a 96-well plate, or $2 × 10^6$ cells per ml in suspension) were sensitized with anti-DNP IgE as described above. Multivalent ligand DNP-BSA (final concentration 100 ng/ml) was added as the stimulus, and cellular degranulation was quantified with a β-hexosaminidase colorimetric assay (35). Degranulation was expressed as a percentage of the total β-hexosaminidase released from cells after lysis with 0.1% Triton X-100.

Measurement of Intracellular Ca^{2+} Mobilization. Cells were loaded with Indo-1 AM (Molecular Probes), and fluorescence was measured on an SML 8100S fluorometer in a time-based acquisition mode as described in ref. 23. The maximum fluorescence from each sample was measured after lysing cells with 0.1% Triton X-100. Background fluorescence was measured by adding EDTA to the buffer. The Ca^{2+} response was quantified by using a normalization factor for each condition as described in ref. 23.

1. Lock JG, Wehrle-Haller B, Stromblad S (2008) Cell–matrix adhesion complexes: Master control machinery of cell migration. *Semin Cancer Biol* 18:65–76.
2. Kinet J-P (1999) The high-affinity IgE receptor (FcεRI): From physiology to pathology. *Annu Rev Immunol* 17:931–972.
3. Holowka D, *et al.* (2005) Lipid segregation and IgE receptor signaling: A decade of progress. *Biochim Biophys Acta* 1746:252–259.
4. Wu M, Holowka D, Craighead HG, Baird B (2004) Visualization of plasma membrane compartmentalization with patterned lipid bilayers. *Proc Natl Acad Sci USA* 101:13798–13803.
5. Critchley DR (2000) Focal adhesions: The cytoskeletal connection. *Curr Opin Cell Biol* 12:133–139.
6. Brown MC, Turner CE (2004) Paxillin: Adapting to change. *Physiol Rev* 84:1315–1339.
7. Hamawy MM, *et al.* (1994) The aggregation of the high affinity IgE receptor induces tyrosine phosphorylation of paxillin, a focal adhesion protein. *J Immunol* 153:4655–4662.
8. Minoguchi KKH, Nishikata H, Hamawy MM, Siraganian RP (1994) Src family tyrosine kinase Lyn binds several proteins including paxillin in rat basophilic leukemia cells. *Mol Immunol* 31:519–529.
9. Bretscher A, Edwards K, Fehon RG (2002) ERM proteins and merlin: Integrators at the cell cortex. *Nat Rev Mol Cell Biol* 3:586–599.
10. Ilani T, Khanna C, Zhou M, Veenstra TD, Bretscher A (2007) Immune synapse formation requires ZAP-70 recruitment by ezrin and CD43 removal by moesin. *J Cell Biol* 179:733–746.

11. Gehlsen KR, Argraves WS, Pierschbacher MD, Ruoslahti E (1988) Inhibition of *in vitro* tumor cell invasion by Arg-Gly-Asp-containing synthetic peptides. *J Cell Biol* 106:925–930.

12. El-Hillal O, Kurosaki T, Yamamura H, Kinet JP, Scharenberg AM (1997) Syk kinase activation by a src kinase-initiated activation loop phosphorylation chain reaction. *Proc Natl Acad Sci USA* 94:1919–1924.

13. Lai JYQ, *et al.* (2003) Potent small molecule inhibitors of spleen tyrosine kinase (Syk). *Bioorg Med Chem Lett* 13:3111–3114.

14. Sheets ED, Holowka D, Baird B (1999) Critical role for cholesterol in Lyn-mediated tyrosine phosphorylation of FcεRI and their association with detergent-resistant membranes. *J Cell Biol* 145:877–887.

15. Honda Z-i, *et al*. (1997) Roles of C-terminal Src kinase in the initiation and the termination of the high affinity IgE receptor-mediated signaling. *J Biol Chem* 272:25753–25760.

16. Torres AJ, Wu M, Holowka D, Baird B (2008) Nanobiotechnology and cell biology: Micro- and nanofabricated surfaces to investigate receptor-mediated signaling. *Annu Rev Biophys* 37:265–288.

17. Orth RN, Wu M, Holowka DA, Craighead HG, Baird BA (2003) Mast cell activation on patterned lipid bilayers of subcellular dimensions. *Langmuir* 19:1599–1605.

18. Kam L, Boxer SG (2001) Cell adhesion to protein-micropatterned-supported lipid bilayer membranes. *J Biomed Mater Res* 55:487–495.

19. Frigeri L, Apgar JR (1999) The role of actin microfilaments in the down-regulation of the degranulation response in RBL-2H3 Mast Cells. *J Immunol* 162:2243–2250.

20. Holowka D, Sheets ED, Baird B (2000) Interactions between FcεRI and lipid raft components are regulated by the actin cytoskeleton. *J Cell Sci* 113:1009–1019.

21. Oka T, Sato K, Hori M, Ozaki H, Karaki H (2002) FcεRI cross-linking-induced actin assembly mediates calcium signalling in RBL-2H3 mast cells. *Br J Pharmacol* 136:837–846.

22. Torigoe C, Song J, Barisas BG, Metzger H (2004) The influence of actin microfilaments on signaling by the receptor with high affinity for IgE. *Mol Immunol* 41:817–829.

23. Pierini L, Harris NT, Holowka D, Baird B (1997) Evidence supporting a role for microfilaments in regulating the coupling between poorly dissociable IgE-FcεRI aggregates and downstream signaling pathways. *Biochemistry* 36:7447–7456.

24. Ziegler WH, Liddington RC, Critchley DR (2006) The structure and regulation of vinculin. *Trends Cell Biol* 16:453–460.

25. Rathore VB, Okada M, Newman PJ, Newman DK (2007) Paxillin family members function as Csk-binding proteins that regulate Lyn activity in human and murine platelets. *Biochem J* 403:275–281.

26. Chew V, Lam K-P (2007) Leupaxin negatively regulates B cell receptor signaling. *J Biol Chem* 282:27181–27191.

27. Ra CYM, Yagita H, Okumura K (1994) Fibronectin receptor integrins are involved in mast cell activation. *J Allergy Clin Immunol* 94:625–628.

28. Krüger-Krasagakes K, Grützkau A, Krasagakis K, Hoffmann S, Henz BM (1999) Adhesion of human mast cells to extracellular matrix provides a costimulatory signal for cytokine production. *Immunology* 98:253–257.

29. Hamawy MM, Oliver C, Mergenhagen SE, Siraganian RP (1992) Adherence of rat basophilic leukemia (RBL-2H3) cells to fibronectin-coated surfaces enhances secretion. *J Immunol* 149:615–621.

30. Wyczolkowska JDJ, Slusarczyk A, Kolago B (1994) Relations between FcεRI cross-linking-induced mast cell activation and adhesion to fibronectin. *J Physiol Pharmacol* 45:501–516.

31. Dastych J, Wyczólkowska J, Metcalfe DD (2001) Characterization of α5-integrin-dependent mast cell adhesion following FcεRI aggregation. *Int Arch Allergy Immunol* 125:152–159.

32. Odom S, *et al*. (2004) Negative regulation of immunoglobulin E-dependent allergic responses by Lyn kinase. *J Exp Med* 199:1491–1502.

33. Subramanian K, Holowka D, Baird B, Goldstein B (1996) The Fc segment of IgE influences the kinetics of dissociation of a symmetrical bivalent ligand from cyclic dimeric complexes. *Biochemistry* 35:5518–5527.

34. Pierini L, Holowka D, Baird B (1996) FcεRI-mediated association of 6-micron beads with RBL-2H3 mast cells results in exclusion of signaling proteins from the forming phagosome and abrogation of normal downstream signaling. *J Cell Biol* 134:1427–1439.

35. Naal RMZG, Tabb J, Holowka D, Baird B (2004) *In situ* measurement of degranulation as a biosensor based on RBL-2H3 mast cells. *Biosens Bioelectr* 20:791–796.